applied sciences

MDPI

Article

The Chloroform Extracts of Vietnamese *Sophora flavescens* Ait. Inhibit the Proliferation of HepG2 Cells through Apoptosis Induction

Cao Ngoc Minh Trang [1,2], Ho Nguyen Quynh Chi [2,3], Nguyen Khac Manh [4], Hoang Nghia Son [2,3], Dai-Nghiep Ngo [5,6,*] and Le Thanh Long [2,3,*]

1 Faculty of Applied Technology, School of Engineering and Technology, Van Lang University, Ho Chi Minh City 700000, Vietnam; trang.caongocminh@hotmail.com
2 Biotechnology Department, Graduate University of Science and Technology, Vietnam Academy of Science and Technology, Ha Noi 100000, Vietnam; quynhchihonguyen@gmail.com (H.N.Q.C.); hoangnghiason@yahoo.com (H.N.S.)
3 Animal Biotechnology Department, Institute of Tropical Biology, Vietnam Academy of Science and Technology, Ho Chi Minh City 700000, Vietnam
4 Institute for Tropical Technology and Environmental Protection, Ho Chi Minh City 700000, Vietnam; manhnk.tt@gmail.com
5 Department of Biochemistry, Faculty of Biology—Biotechnology, University of Science, Ho Chi Minh City 700000, Vietnam
6 Faculty of Biology—Biotechnology, Vietnam National University Ho Chi Minh City, Ho Chi Minh City 700000, Vietnam
* Correspondence: ndnghiep@hcmus.edu.vn (D.-N.N.); longlt@itb.ac.vn (L.T.L.)

Abstract: The present study evaluated the effects of *Sophora flavescens* Ait. root extract on the proliferation of human hepatoma cell line HepG2. HPLC-UV analysis showed that the highest matrine and oxymatrine contents were obtained in the chloroform extract, compared to ethanol extract and ethyl acetate extract. The morphological analysis revealed that the chloroform extract of *Sophora flavescens* Ait. (SFA-CHCl3 extract) induced alterations of HepG2 cell morphology, resulting in the shrinkage of cells, the formation of debris, and cell detachment. The proliferation of HepG2 cells was inhibited by SFA-CHCl3 extract treatment. Cell cycle analysis exhibited that the cell proportion of the G0/G1 phase of HepG2 cells with SFA-CHCl3 extract treatment was decreased, while the cell proportion of the G2/M phase was increased. Flow cytometry analysis indicated a dramatic increase in the apoptotic percentage of HepG2 cells over the time of SFA-CHCl3 extract treatment. The SFA-CHCl3 extract also caused morphological changes in HepG2 nuclear, including chromatin condensation and DNA fragmentation. SFA-CHCl3 extract treatment induced the bax up-regulation and the bcl-2 down-regulation in HepG2 cells. These results revealed that SFA-CHCl3 extract could be a potential apoptosis inducer in HepG2 cells.

Keywords: apoptosis; HepG2 cells; proliferation; *Sophora flavescens* Ait

Citation: Trang, C.N.M.; Chi, H.N.Q.; Manh, N.K.; Son, H.N.; Ngo, D.-N.; Long, L.T. The Chloroform Extracts of Vietnamese *Sophora flavescens* Ait. Inhibit the Proliferation of HepG2 Cells through Apoptosis Induction. *Appl. Sci.* **2022**, *12*, 5906. https://doi.org/10.3390/app12125906

Academic Editor: Monica Gallo

Received: 26 April 2022
Accepted: 7 June 2022
Published: 10 June 2022

1. Introduction

Liver cancer has remained a world health challenge. The most common kind of liver cancer is hepatocellular carcinoma (HCC), accounting for 90% of all occurrences [1]. HCC can be treated effectively using a number of therapies such as resection, liver transplantation, chemoembolization, and systemic medicines. Additionally, the use of herbal medicine in the treatment of liver cancer has also been documented. The Chinese and English medical literature have reported that herbal medicine could be useful in the treatment of HCC [2]. In addition, network pharmacology investigates the components, targets, and synergistic connections between drugs, targets, and diseases. These findings are applied to explain pharmacological activity [3]. Network pharmacology has enabled herbal

medicine researchers to look beyond a single ingredient, target, or condition to investigate the effectiveness of herbal medicine and its mechanisms [4].

Apoptosis, a form of programmed cell death, is considered an anti-cancer mechanism (Pistritto et al., 2016) [5]. Apoptotic cells exhibit morphological changes including cytoplasmic shrinkage, plasma membrane budding, exposure of phosphatidylserine on the extracellular side, chromatin condensation, and DNA fragmentation (Hacker, 2000) [6]. Apoptosis can be triggered by both intrinsic and extrinsic factors (Pfeffer 2018; Al-Aamri et al., 2021) [7,8]. Many anti-tumor drugs can target different stages of intrinsic and extrinsic pathways (Liu 2017) [9]. Nowadays, some herbal medicine has been shown to be useful in cancer treatment by triggering apoptosis (Li 2022) [10].

Sophora flavescens is a medicinal plant that has recently received a lot of attention. *Sophora flavescens* is a plant that could be used for removing heat and humidity from the body, as well as killing insects [11]. Kushen, a dried stem of *Sophora flavescens*, has been demonstrated in clinical testing to have low toxicity and negative effects [12]. Kushen has shown several therapeutic effects, including swelling reduction, immunostimulation, and anti-tumor properties [13]. *Sophora flavescens* contains a variety of pharmacological activity compounds such as matrine alkaloids, flavonoids, and the saponin sophoraflavoside [14]. These compounds also exhibit anti-oxidant and anti-cancer properties [15,16]. A recent study showed that the compounds from *Sophora flavescens* exhibit anti-oxidant properties and proliferative inhibition in several cell lines (HepG2, A549, and MCF7) [16]. The prenylated flavanonol from *Sophora flavescens* could inhibit HeLa and HL-60 tumor cell lines [17]. However, the mechanism of inhibited proliferation in HepG2 cells induced by SFA extracts has not been well characterized. Therefore, this study was conducted to estimate the capacity of matrine and oxymatrine-rich extracts of *Sophora flavescens* in proliferative inhibition, as well as their ability to induce apoptosis in HepG2 cells.

2. Materials and Methods

2.1. Extraction and Fractionation

Sophora flavescens Ait. samples were collected from Dak Nong Province, Vietnam (Figure 1). Pharmaceutical powder characterization was performed following Chinese Pharmacopoeia 2010 (Figures S1 and S2). *Sophora flavescens* roots were air-dried to dryness at room temperature, then powdered and used for fraction extraction. The dried and powdered sample (100 g) was successively extracted with an ethanol–water mixture (80:20 v/v) at 50 °C for 24 h using an IKA RW20 impeller (IKA, Staufen, Germany) apparatus at 500 rpm. The solvent was then removed under reduced pressure to obtain sticky residues. The crude ethanol extract, after the removal of the solvent, was dispersed in water and partitioned with ethyl acetate and chloroform successively to give ethyl acetate, chloroform, and water-soluble fractions.

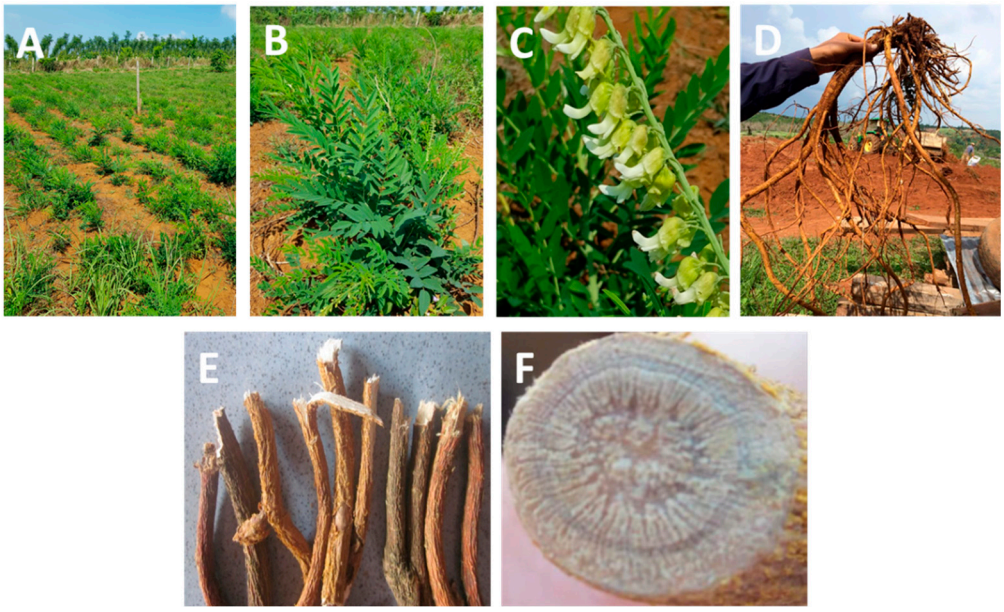

Figure 1. SFA samples. (**A**) SFA was cultivated in Dak Nong province, Vietnam. (**B**) SFA tree. (**C**) SFA flowers. (**D**) SFA roots. (**E**) SFA dry root samples. (**F**) Transverse section of SFA root.

2.2. Solid-Phase Extraction and Prep-HPLC Separation

The solid-phase extraction (SPE) procedure was performed under the modified method, which was described by Bi and colleagues [18]. This experiment performed SPE on a chloroform fraction extract (1 g) of SFA roots, and the purity extracts were reconstituted in 50% methanol. Before the elution, each mixed-mode polymeric sorbent cartridge (OASIS- MCX 6 cc, 150 mg, Waters Corp., Milford, MA, USA) was pre-activated with 10 mL methanol and distilled water to eliminate any impurities. The sample's methanol solution was fractionated on the cartridge and eluted with 3 mL of 5% ammonia solution in methanol. Following the OASIS MCX cartridge's partial separation, a rotary evaporator was used to dry the collected fractions at 30 °C, and a speed vacuum concentrator was used at 30 °C. A modified method was applied to perform prep-HPLC separation [19]. Prep-HPLC was performed with a Shimadzu UFLC system with a reversed-phase C18 column (250 mm × 21.2 mm, i.d., 10 µm particle size, Supelco Japan). The mobile phase produced solvent A (5% aqueous acetonitrile) and solvent B (100% acetonitrile). The mobile phase at a flow of 10 mL·min^{-1} was made up of 0.1% formic acid in water (phase A) and 0.1% formic acid in acetonitrile (phase B). A gradient of solvents was applied as follows: 0–15 min: 7.5–90% phase B, 15.1–19 min: 100% phase B, and finally, 19.1–25 min: 7.5% phase B, maintained for 10 min before each new injection. A 220 nm wavelength was used to monitor each injection. The contents of the matrine and oxymatrine fractions were collected and dried using a rotary evaporator at 30 °C. HRESIMS data were obtained from a Bruker micrOTOF—QII mass spectrometer (Berlin, Germany). The quantitation of matrine and oxymatrine was carried out using an Agilent 1200 Infinity chromatograph coupled with a UV detector (Agilent Technologies Co., Ltd., Santa Clara, CA, USA) with an Eclipse XDB—C18 column (4.6 × 250 mm, 5 µm) from Agilent (Santa Clara, CA, USA).

2.3. Cell Culture and SFA Extract Treatment

HepG2 cells were purchased from the American Type Culture Collection (ATCC, Manassas, VA, USA). The cell culture medium was DMEM/Ham's F-12 (DMEM-12-A, Capricorn Scientific, Ebsdorfergrund, Germany), containing 15% fetal bovine serum (FBS-HI-22B, Capricorn Scientific, Ebsdorfergrund, Germany) and 1% antibiotics (15140-122, Gibco, Thermo Fisher Scientific, Waltham, MA, USA). HepG2 cells in the experimental groups were exposed to 3.125, 6.25, 12.5, 25, 50, and 100 µg/mL SFA-CHCl3 extract for 48 h.

The IC_{50} value was determined and used to assess the proliferation and viability of HepG2 cells for 24 h, 48 h, and 72 h of SFA-CHCl3 extract treatment.

2.4. Cell Density Determination

The cells were seeded in 96-well plates (Thermo Fisher Scientific, Waltham, MA, USA) with a density of 5×10^3 cells/well. After SFA-CHCl3 extract treatment, cells were washed in PBS solution and 100 µL of culture media were added to each well. An amount of 10 µL WST-1 (11644807001, Roche, Basel, Switzerland) was added to each well, and HepG2 cells were incubated for 3.5 h at 37 °C, 5% CO_2. GloMax® Explorer Multimode Microplate Reader (Promega Corporation, Fitchburg, WI, USA) was applied to measure the O.D. value at 450 nm wavelength. The standard curve was performed by determining the O.D. values of cells at different densities (5×10^2, 1×10^3, 5×10^3, 1×10^4, 5×10^4 cells/well). The standard curve was applied to calculate the cell density in the experimental groups.

2.5. Flow Cytometry Analysis

Flow cytometry analysis was applied to estimate the apoptosis and cycle progression of HepG2 cells under SFA-CHCl3 extract treatment at 24 h, 48 h, and 72 h. The cells were seeded in T25 tissue culture flasks (160430, Thermo Fisher Scientific, Waltham, MA, USA) at 1×10^5 cells/flask density. The apoptosis analysis was executed using an Apoptosis Detection Kit I (556547, BD Biosciences, San Jose, CA, USA) in Accuri C6 Plus flow cytometer (BD Biosciences, San Jose, CA, USA). In cell cycle analysis, 4% paraformaldehyde (09154-85, Nacalai Tesque, Kyoto, Japan) was used for fixing the cell. Cell nuclear were then stained with 5 µL propidium iodide (51-66211E, BD Biosciences, San Jose, CA, USA). The cell cycle progression was subsequently analyzed using a flow cytometer.

2.6. Nuclear Staining

Cell fixation was performed with 4% paraformaldehyde (Nacalai Tesque, Kyoto, Japan) for 30 min; then, 0.1% Triton X-100 was used to permeabilize the fixed cells (Merck, Darmstadt, Germany) overnight at 4 °C. Nuclear staining was carried out with 2 µg/mL Hoechst 33342 solution (14533, Sigma-Aldrich, Munich, Germany) for 15 min at room temperature. Phosphate-buffered saline (Gibco, Thermo Fisher Scientific, Waltham, MA, USA) was used for cell washing for 10 min each. The nuclear morphology was evaluated under a Cytell fluorescent microscope (GE Healthcare, Chicago, IL, USA).

2.7. Real-Time RT-PCR

RNA extraction was performed with ReliaPrepTM RNA Cell Miniprep kit (Promega Corporation, Madison, WI, USA). Real-time quantitative RT-PCR was carried out using a PikoReal System (Thermo Fisher Scientific, Waltham, MA, USA) and a 2× qPCR SyGreen 1-Step kit (PCRBiosystems, London, UK). The PCR reaction was performed as follows: one cycle of 45 °C for 15 min; heating to 95 °C for 2 min; 40 cycles of 95 °C for 10 s; 60 °C for 15 s; and 71 cycles of 60 °C for 15 s. Primers were as follows: bax, F: 5′-CTT TTG CTT CAG GGT TTC ATC-3′ and R: 5′-CAC TCG CTC AGC TTC TTG GT-3′; bcl-2, F: 5′-TTC TTT GAG TTC GGT GGG G-3′ and R: 5′-CAG GAG AAA TCA AAC AGA GGC-3′; gapdh, F: 5′-GAA GGT CGG AGT CAA CGG ATT T-3′ and R: 5′-CTG GAA GAT GGT GAT GGG ATT TC-3′ [20]. The relative expression of these genes was analyzed using the $2^{-\Delta\Delta Ct}$ method [21].

2.8. Western Blot

The HepG2 cells were lysed with the Lysis buffer (ab119196, Abcam, Cambridge, MA, USA). The protein samples were loaded into Precast Gel SDS-PAGE 4–12% (ab139596, Abcam, Cambridge, MA, USA) with an equal amount for each well. Gel electrophoresis was performed with running buffer (ab119197, Abcam, Cambridge, MA, USA) for 2 h at 50 V. The proteins were transferred to a methanol-activated PVDF membrane (ab133411, Abcam, Cambridge, MA, USA). Blocking buffer (ab126587, Abcam, Cambridge, MA, USA) was applied to blocking membrane overnight at 4 °C. The primary antibody incubation

was carried out overnight at 4 °C. Anti-Bax antibody (ab53154, Abcam, Cambridge, MA, USA) and Anti-bcl-2 antibody (ab196495, Abcam, Cambridge, MA, USA) were employed at the 1/5000 dilution. Anti-GAPDH antibody (ab181602, Abcam, Cambridge, MA, USA) was employed as the control at the 1/10,000 dilution. The membrane was washed using TBST solution and incubated with Goat Anti-Rabbit IgG (HRP) (ab6721, Abcam, Cambridge, MA, USA) for 1 h at room temperature. Blot visualization was conducted using an ECL Substrate Kit (ab65623, Abcam, Cambridge, MA, USA) and X-ray film.

2.9. Statistical Analysis

The results were presented as mean ± standard deviation. One-way ANOVA was applied to analyze the statistical significance, where $p < 0.05$ was considered statistically significant.

3. Results

3.1. SFA Extraction

Table 1 demonstrates the matrine and oxymatrine contents from different extracts of SFA powder. The chloroform extract showed higher matrine and oxymatrine contents than ethanol extract and ethyl acetate extract. Matrine and oxymatrine contents were not detected in the aqueous extract.

Table 1. Matrine and oxymatrine contents.

Solvent	Matrine (mg/g)	Oxymatrine (mg/g)
Ethanol extract	28.1	1.79
Chloroform extract	70.1	4.2
Ethyl acetate extract	1.1	0.09
Aqueous extract	ND	ND

3.2. Effects of SFA-CHCl3 Extract on HepG2 Cell Morphology

The morphology of the HepG2 cells in the control group and the SFA-CHCl3 extract-treated groups were evaluated by observation under a microscope. The treatment with 3.125 μg/mL, 6.25 μg/mL, and 12.5 μg/mL SFA-CHCl3 extract did not result in morphological changes in HepG2 cells (Figure 2A–C). An amount of 25 μg/mL SFA-CHCl3 extract treatment induced the morphological alteration in HepG2 cells (Figure 2D). The treatment with 50 μg/mL and 100 μg/mL SFA-CHCl3 extract caused marked morphological alterations of HepG2 cells, demonstrated by the shrinkage and detachment of cells (Figure 2E,F). These results showed that the SFA-CHCl3 extract treatment induced morphological changes in HepG2 cells.

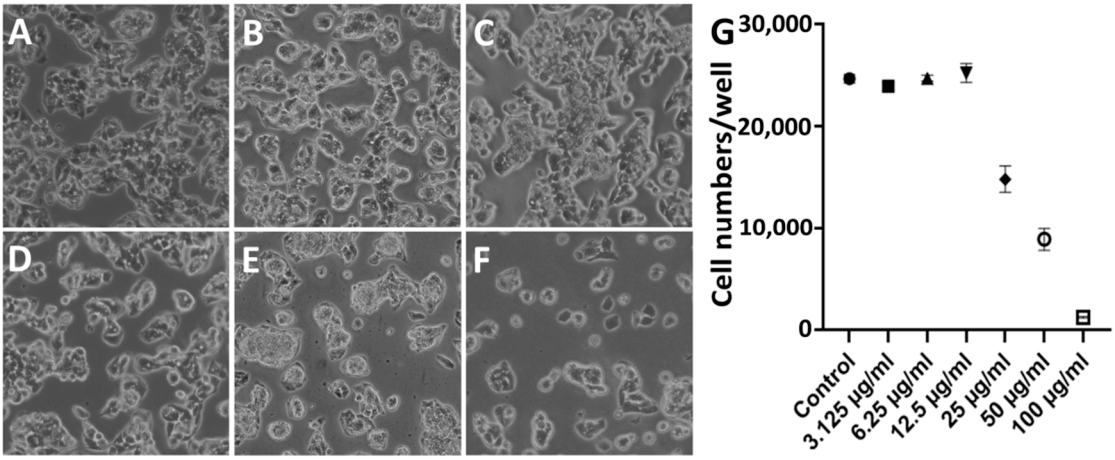

Figure 2. Morphological alterations of HepG2 cells under SFA-CHCl3 extract treatment. HepG2 cells from the treatment of 3.125 μg/mL (**A**), 6.25 μg/mL (**B**), and 12.5 μg/mL (**C**) SFA-CHCl3 extract

showed normal morphology. HepG2 cells showed morphological changes in 25 μg/mL (**D**), 50 μg/mL (**E**), and 100 μg/mL (**F**) SFA-CHCl3 extract groups. (**G**) Cell density was analyzed by WST-1 assay. Original magnification 100×.

3.3. Effects of SFA-CHCl3 Extract on HepG2 Cell Proliferation

As seen in Figure 2G, there was no statistical difference in cell density between the control group and the 3.125 μg/mL, 6.25 μg/mL, and 12.5 μg/mL SFA-CHCl3 extract treatment groups (2.47×10^4/well vs. 2.39×10^4/well, 2.47×10^4/well, and 2.52×10^4/well, respectively). The cell density of the 25 μg/mL SFA-CHCl3 extract treatment group was decreased to 1.48×10^4/well. The 50 μg/mL and 100 μg/mL SFA-CHCl3 extract treatment groups showed a dramatic reduction in the cell density of HepG2 cells (0.88×10^4/well and 0.12×10^4/well, respectively). These results indicated that the SFA-CHCl3 extract treatment attenuated the proliferation of HepG2 cells. The IC_{50} value was calculated after 2 days of SFA-CHCl3 extract treatment. The IC_{50} value was calculated as 47.68 μg/mL SFA-CHCl3 extract in HepG2 cells (Figure S3, Tables S1–S3). This value was applied to assess the effects of the SFA-CHCl3 extract on HepG2 cell proliferation over time.

3.4. Effects of SFA-CHCl3 Extract on Cell Cycle Progression of HepG2 Cells

Flow cytometry was also performed to estimate the effects of the SFA-CHCl3 extract treatment on cell cycle progression in HepG2 cells. As shown in Figure 3, the SFA-CHCl3 extract treatment reduced the cell ratio in the G0/G1 phase for 24 h, 48 h, and 72 h, compared to the control group (90.53 ± 0.15%, 87.40 ± 0.23, 85.43 ± 0.58 vs. 91.67 ± 0.55%, respectively) (Figure 3A,B). In contrast, the increase in the cell ratio in the G2/M phase was observed in cell cycle distribution maps. The G2/M phase proportion of HepG2 cells was increased from the control group (2.87 ± 0.06%) to the SFA-CHCl3 extract treatment group for 24 h, 48 h, and 72 h (3.87 ± 0.06%, 6.26 ± 0.31%, and 8.23 ± 0.22%). This result revealed that the SFA-CHCl3 extract treatment induced the G2/M phase arrest of HepG2, which resulted in the inhibition of HepG2 cell proliferation.

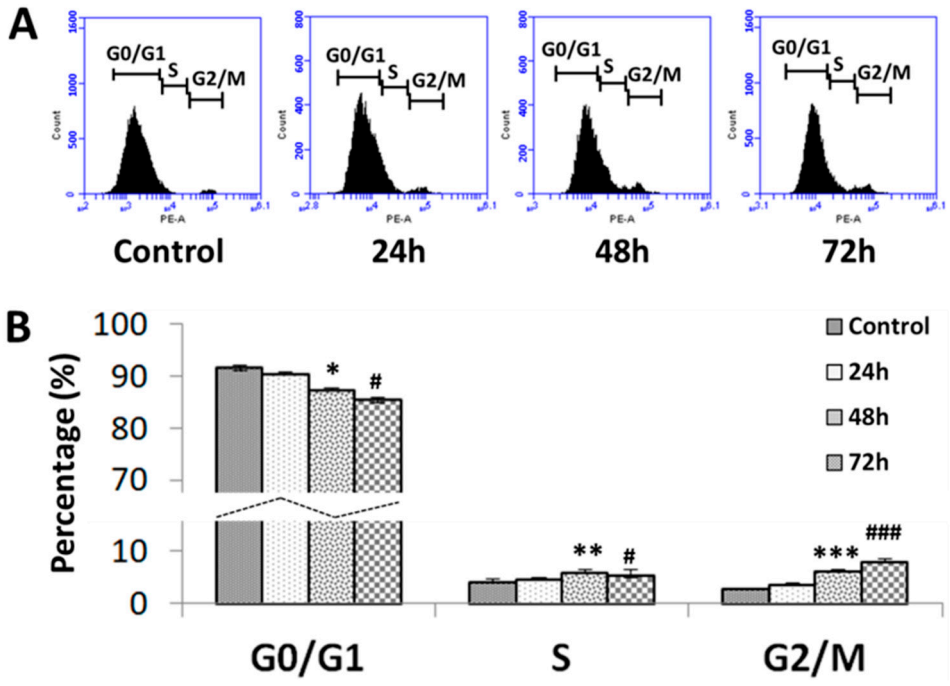

Figure 3. Cycle progression of HepG2 cells over the time of SFA-CHCl3 extract treatment. (**A**) Flow cytometry was applied to analyze the cell cycle progression. (**B**) The calculation of percentage of HepG2 cells in cell cycle phases. The percentage of HepG2 cells in G0/G1 phase was reduced from

24 h to 72 h (* $p < 0.05$, 48 h group vs. other groups; # $p < 0.05$, 72 h group vs. other groups). The percentage of HepG2 cells in S phase was slightly increased in 48 h and 72 h (** $p < 0.01$, 48 h group vs. control group and 24 h group; # $p < 0.05$, 72 h group vs. control group and 24 h group). The percentage of HepG2 cells in G2/M phase was increased in 48 h and 72 h (*** $p < 0.001$, 48 h group vs. other groups; ### $p < 0.001$, 72 h group vs. other groups).

3.5. SFA-CHCl3 Extract Induced Apoptosis of HepG2 Cells

The apoptotic induction of HepG2 cells using SFA-CHCl3 extract treatment was analyzed further by flow cytometry analysis (Figure 4A–D). The increase in SFA-CHCl3 extract treatment time caused a decrease in the live cell ratio. The ratio of cells suffering from apoptosis (including early apoptosis and late apoptosis) was increased from 1.27 ± 0.23% (control group) to 22.90 ± 0.76%, 34.90 ± 1.41%, 43.17 ± 0.67%, after 24 h, 48 h, and 72 h SFA-CHCl3 extract treatment, respectively. Moreover, HepG2 cells under SFA-CHCl3 extract treatment exhibited chromatin condensation and DNA fragmentation (Figure 4E). These results show that SFA-CHCl3 extract treatment could induce significant apoptosis in HepG2 cells.

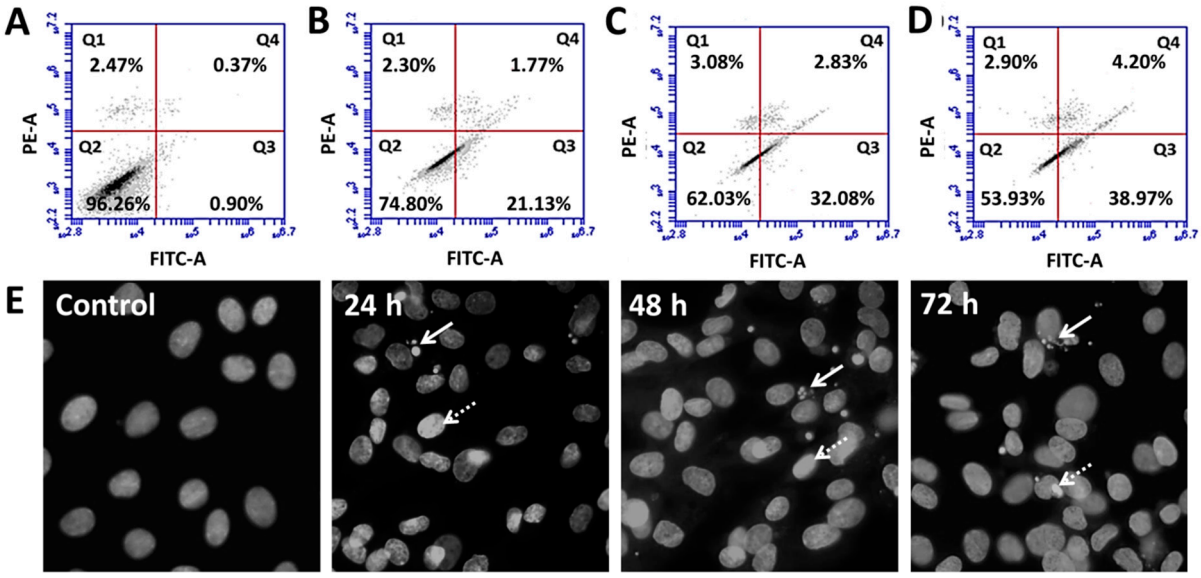

Figure 4. The apoptosis analysis of HepG2 cells over time. (**A**–**D**) displayed the representative apoptosis map of HepG2 cells from control group, 24 h, 48 h, and 72 h of SFA-CHCl3 extract treatment, respectively (Q1 indicates necrotic cells, Q2 indicates the live cells, Q3 indicates the early apoptotic cells, and Q4 indicates the late apoptotic cells). (**E**) Nuclear morphology of HepG2 cells (White arrow indicates nuclear fragmentation; dotted arrow indicates chromatin condensation). Original magnification 400×.

The expression of bax and bcl-2 was determined by real-time RT-PCR and Western blotting (Figure 5A,B). The results showed that bax expression in HepG2 cells under 24 h and 48 h of SFA-CHCl3 extract treatment was higher than HepG2 at 0 h treatment. In contrast, bcl-2 expression was reduced in HepG2 cells for 48 h of SFA-CHCl3 extract treatment, compared to other groups.

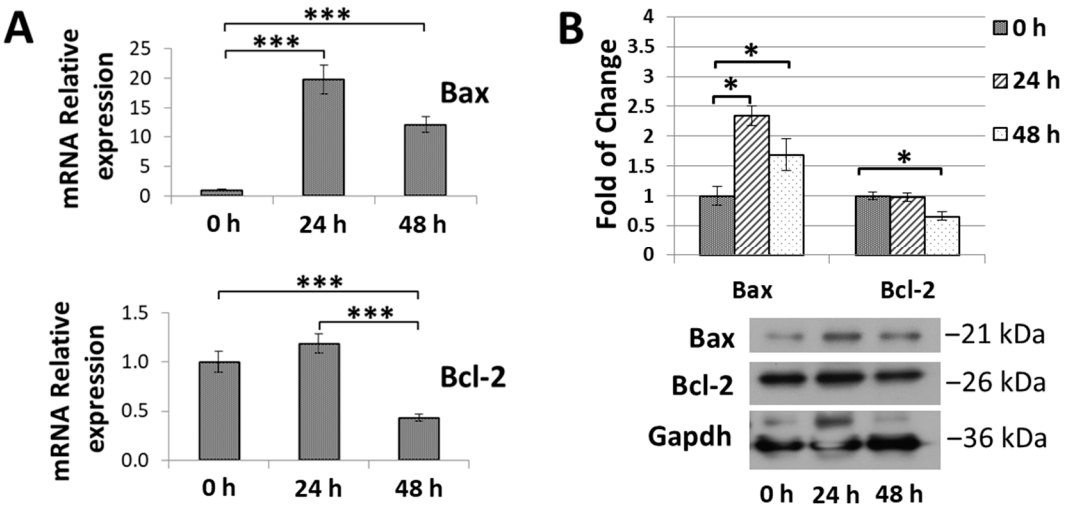

Figure 5. The expression of bax and bcl-2 gene. (**A**) The transcript expression of bax and bcl-2 was performed by real-time RT-PCR, *** indicates significant difference between groups ($p < 0.001$). (**B**) Western blot was applied to estimate the expression of bax and bcl-2. * indicates significant difference between groups ($p < 0.05$).

4. Discussion

HepG2 cell is the most commonly utilized human hepatoma cell line in pharmacotoxicological research [22]. HepG2 cells are highly proliferative and successfully cultured in large-scale systems. When grown on a solid surface, HepG2 cells exhibit an epithelial appearance, and their polarization can arise with the formation of bile canaliculi-like structures between adjacent cells [23,24]. Anti-cancer drugs often suppress cancer cells by apoptotic induction [25,26]. Apoptotic cells exposed several distinguishing characteristics such as cell shrinkage, the condensation of chromatin, nuclear DNA fragmentation, phosphatidylserine expression, and plasma membrane blebbing [27,28]. In this study, HepG2 cells maintained epithelial appearance in the low SFA-CHCl3 extract-treated groups. However, morphological changes in HepG2 cells were observed in the high SFA-CHCl3 extract-treated groups (50 μg/mL and 100 μg/mL SFA-CHCl3 extract), concluding the shrinkage of cells, the formation of debris, and the visible loss of contact and rounding of cell shape that are classic morphologies of apoptosis [29]. Moreover, the SFA-CHCl3 extract treatment at IC_{50} value also resulted in the morphological changes of nuclear in HepG2 cells at 24, 48, and 72 h. These alterations were demonstrated by the nuclear condensation and fragmented nuclear, which are also unique features during apoptosis [30]. Therefore, SFA-CHCl3 extract treatment induced the morphologic hallmarks of apoptosis, by a series of typical morphological events in the cytoplasm and nuclear in HepG2 cells.

These findings suggest that SFA-CHCl3 extract treatment has strong cytotoxicity against HepG2 cells and can limit their proliferation. Cell proliferation is a fundamental process in multi-cellular organisms, and it has been reported to be linked to apoptosis [31]. Uncontrolled proliferation can be associated with a high level of apoptosis. This investigation showed that SFA-CHCl3 extract treatment markedly decreased the proliferation of HepG2 cells in a dose-dependent manner. This reduced proliferation was found to be associated with HepG2 cells from the high SFA-CHCl3 extract-treated groups, which strongly exposed the morphological features of apoptosis.

Cell cycle dysregulation is known to be characteristic of tumor cells. Anti-cancer drugs induce apoptosis by stopping the cell cycle progression in the G1, S, or G2/M stages [27,32,33]. In this study, flow cytometry demonstrated that the percentage of the G0/G1 phase of HepG2 cells under SFA-CHCl3 extract treatment decreased with the increase in time of the treatment, while the percentage of the G2/M phase increased. This result disclosed that SFA-CHCl3 extract treatment significantly arrested the cell cycle of HepG2 cells at the G2/M phase, leading to the inhibited proliferation of HepG2 cells.

Phosphatidylserine exposure on the plasma membrane's outer leaflet is a common alteration in apoptotic cells, and it has been considered a unique feature of these cells [34,35]. This marker can be detected by double-staining with annexin V and PI; flow cytometry analysis revealed a dramatic increase in the apoptotic percentage of HepG2 cells, suggesting that SFA-CHCl3 extract could induce significant apoptosis in HepG2 cells.

The Bcl2 family plays a key role in intrinsic mitochondrial apoptosis [36]. Bcl2 interacts with pro-apoptotic proteins such as Bax, limiting pore development and the release of cytochrome c [37]. On the other hand, an increase in Bax expression causes tumor cells to die, resulting in cell death [38]. The present investigation showed that bax up-regulation and bcl-2 down-regulation were determined in HepG2 cells under SFA-CHCl3 extract treatment. This revealed that SFA-CHCl3 extract could induce apoptosis in HepG2 cells by intrinsic pathway.

Previous studies have shown that treatment with matrine and oxymatrine induces inhibition of tumor cell proliferation in different types of cancer, including breast cancer [39], colon cancer [40], melanoma [41], glioma [42], pancreatic cancer [43], and hepatoma [44]. Treatment with matrine showed inhibition of HepG2 cell proliferation [45,46]. Oxymatrine inhibits the proliferation and induces apoptosis of human hepatoma SMMC-7721 cells [44]. Moreover, oxymatrine has been shown to inhibit the migration and invasion of human HCC cell line MHCC97H [47]. However, the effects of a combination of matrine and oxymatrine on tumor cells have not been well characterized. Combinations of bioactive compounds play an important role in traditional medicines, particularly Sophora flavescens, because the extracts are often composed of many compounds that act synergistically to inhibit proliferation or induce apoptosis in cancer cells. In this study, we found that SFA-CHCl3 extract showed a high content of matrine and oxymatrine. In addition, SFA-CHCl3 extract treatment resulted in effectively suppressing HepG2 cell proliferation through apoptosis.

5. Conclusions

This study showed the potential of SFA-CHCl3 extract in the proliferative inhibition of HepG2 cells by inducing apoptosis. Further studies should be performed to evaluate the effects of SFA-CHCl3 extract on in vivo suppression of hepatocellular carcinoma to clarify the anti-cancer capacity of SFA-CHCl3 extract.

Supplementary Materials: The following supporting information can be downloaded at: https://www.mdpi.com/article/10.3390/app12125906/s1, Figure S1: Pharmaceutical powder characterization; Figure S2: A cross-section of SFA root; Figure S3: The WST-1 standard curve plotted to estimate the cell number for O.D. values obtained from WST-1 assay; Table S1: O.D. values of HepG2 cells; Table S2: O.D. values of HepG2 cells treated with SFA-CHCl3 extract; Table S3: Cell density of HepG2 cells treated with SFA-CHCl3 extract.

Author Contributions: Conceptualization, H.N.S. and L.T.L.; Data curation, C.N.M.T., N.K.M. and D.-N.N.; Formal analysis, C.N.M.T. and L.T.L.; Investigation, C.N.M.T., H.N.Q.C., D.-N.N. and H.N.S.; Methodology, C.N.M.T., H.N.S. and L.T.L.; Validation, C.N.M.T., H.N.S. and L.T.L.; Visualization, D.-N.N. and H.N.S.; Writing—review and editing, C.N.M.T., H.N.S., D.-N.N. and L.T.L. All authors have read and agreed to the published version of the manuscript.

Funding: This study was supported by VLU_Grant 2022 of Van Lang University, Vietnam.

Institutional Review Board Statement: Not applicable.

Informed Consent Statement: Not applicable.

Data Availability Statement: All data sets obtained and analyzed during the current study are available in the manuscript.

Acknowledgments: The authors thank Van Lang University, Vietnam for funding this work.

Conflicts of Interest: The authors declare no conflict of interest.

Abbreviations

DMEM	Dulbecco's Modified Eagle's Medium
FBS	Fetal bovine serum
GAPDH	Glyceraldehyde-3-phosphate dehydrogenase
HPLC	High-performance liquid chromatography
HRESIMS	High-resolution electrospray ionisation mass spectrometry
HRP	Horseradish peroxidase
IgG	Immunoglobulin G
O.D.	Optical density
PBS	Phosphate-buffered saline
Pen/Strep	Penicillin/streptomycin
PI	Propidium iodide
SDS-PAGE	Sodium dodecyl sulfate polyacrylamide gel electrophoresis
TBST	Tris-buffered saline, 0.1% Tween 20
UFLC	Ultra-fast liquid chromatography

References

1. Llovet, J.M.; Kelley, R.K.; Villanueva, A.; Singal, A.G.; Pikarsky, E.; Roayaie, S.; Lencioni, R.; Koike, K.; Zucman-Rossi, J.; Finn, R.S. Hepatocellular carcinoma. *Nat. Rev. Dis. Primers* **2021**, *7*, 6. [CrossRef] [PubMed]
2. Xi, S.Y.; Minuk, G.Y. Role of traditional Chinese medicine in the management of patients with hepatocellular carcinoma. *World J. Hepatol.* **2018**, *10*, 799–806. [CrossRef] [PubMed]
3. Zhu, N.; Hou, J.; Ma, G.; Liu, J. Network pharmacology identifes the mechanisms of action of Shaoyao gancao decoction in the treatment of osteoarthritis. *Med. Sci. Monit.* **2019**, *25*, 6051–6073. [CrossRef] [PubMed]
4. Zhu, N.; Hou, J. Exploring the mechanism of action Xianlingubao Prescription in the treatment of osteoporosis by network pharmacology. *Comput. Biol. Chem.* **2020**, *85*, 107240. [CrossRef]
5. Pistritto, G.; Trisciuoglio, D.; Ceci, C.; Garufi, A.; D'Orazi, G. Apoptosis as anticancer mechanism: Function and dysfunction of its modulators and targeted therapeutic strategies. *Aging* **2016**, *8*, 603–619. [CrossRef]
6. Hacker, G. The morphology of apoptosis. *Cell Tissue Res.* **2000**, *301*, 5–17. [CrossRef]
7. Pfeffer, C.M.; Singh, A.T.K. Apoptosis: A Target for Anticancer Therapy. *Int. J. Mol. Sci.* **2018**, *19*, 448. [CrossRef]
8. Al-Aamri, H.M.; Irving, H.R.; Bradley, C.; Meehan-Andrews, T. Intrinsic and extrinsic apoptosis responses in leukaemia cells following daunorubicin treatment. *BMC Cancer* **2021**, *21*, 438. [CrossRef]
9. Liu, Y.; Zhu, X. Endoplasmic reticulum-mitochondria tethering in neurodegenerative dieseaes. *Transl. Neurodegener.* **2017**, *6*, 21. [CrossRef]
10. Li, M.; Tang, D.; Yang, T.; Qian, D.; Xu, R. Apoptosis Triggering, an Important Way for Natural Products From Herbal Medicines to Treat Pancreatic Cancers. *Front. Pharmacol.* **2022**, *12*, 796300. [CrossRef]
11. Ding, P.L.; He, C.M.; Cheng, Z.H.; Chen, D.F. Flavonoids rather than alkaloids as the diagnostic constituents to distinguish Sophorae Flavescentis Radix from Sophorae Tonkinensis Radix et Rhizoma: An HPLC fngerprint study. *Chin. J. Nat. Med.* **2018**, *16*, 951–960. [CrossRef]
12. Zhu, N.; Hou, J. Molecular mechanism of the anti-inflammatory effects of Sophorae Flavescentis Aiton identified by network pharmacology. *Sci. Rep.* **2021**, *11*, 1005. [CrossRef] [PubMed]
13. Song, L.Y.; Ma, Y.T.; Fang, W.J.; He, Y.; Wu, J.L.; Zuo, S.R.; Deng, Z.Z.; Wang, S.F.; Liu, S.K. Inhibitory efects of oxymatrine on hepatic stellate cells activation through TGF-beta/miR-195/Smad signaling pathway. *BMC Complement. Altern. Med.* **2019**, *19*, 138. [CrossRef] [PubMed]
14. Aronson, J.K. *Meyler's Side Effects of Drugs*, 16th ed.; Elsevier: Amsterdam, The Netherlands, 2016; pp. 229–236.
15. Qin, X.G.; Hua, Z.; Shuang, W.; Wang, Y.H.; Cui, Y.D. Effects of matrine on HepG2 cell proliferation and expression of tumor relevant proteins in vitro. *Pharm. Biol.* **2010**, *48*, 275–281. [CrossRef]
16. Li, J.; Lin, Y.; He, L.; Ou, R.; Chen, T.; Zhang, X.; Li, Q.; Zeng, Z.; Long, Q. Two New Isoprenoid Flavonoids from *Sophora flavescens* with Antioxidant and Cytotoxic Activities. *Molecules* **2021**, *26*, 7228. [CrossRef]
17. Zhang, Y.Q.; Zhao, F.; Ma, J.X.; Gan, H.Y.; Xie, X.F.; Qiao, Z.L.; Zhao, J. A New Prenylated Flavanonol from the Roots of Sophora flavescens. *Chem. Nat. Compd.* **2021**, *57*, 20–22. [CrossRef]
18. Bi, W.; Tian, M.; Row, K.H. Solid-phase extraction of matrine and oxymatrine from *Sophora flavescens* Ait using amino-imidazolium polymer. *J. Sep. Sci.* **2010**, *33*, 1739–1745. [CrossRef]
19. Tian, M.; Row, K.H. Simultaneous extraction and separation of martrine, sophoridine and sophocarpine from *Sophora flavescens* ait by rp-hplc with analytical and preparative chromatography. *J. Liq. Chromatogr. Relat. Technol.* **2009**, *33*, 259–269. [CrossRef]
20. Chen, Y.; Liu, J.; Yuan, B.; Cao, C.; Qin, S.; Cao, X.; Bian, G.; Wang, Z.; Jiang, J. Methylated actinomycin D, a novel actinomycin D analog induces apoptosis in HepG2 cells through Fas- and mitochondria-mediated pathways. *Mol. Carcinog.* **2013**, *52*, 983–996. [CrossRef] [PubMed]

21. Livak, K.J.; Schmittgen, T.D. Analysis of relative gene expression data using Real-Time Quantitative PCR and the $2^{-\Delta\Delta Ct}$ Method. *Methods* **2001**, *25*, 402–408. [CrossRef]
22. Donato, M.T.; Tolosa, L.; Gómez-Lechón, M.J. Culture and Functional Characterization of Human Hepatoma HepG2 Cells. In *Protocols in In Vitro Hepatocyte Research. Methods in Molecular Biology (Methods and Protocols)*; Vinken, M., Rogiers, V., Eds.; Humana Press: New York, NY, USA, 2015; Volume 1250.
23. Sormunen, R.; Eskelinen, S.; Lehto, V.P. Bile canaliculus formation in cultured HEPG2 cells. *Lab. Investig.* **1993**, *68*, 652–662. [PubMed]
24. Fearn, R.A.; Hirst, B.H. Predicting oral drug absorption and hepatobiliary clearance: Human intestinal and hepatic in vitro cell models. *Environ. Toxicol. Pharmacol.* **2006**, *21*, 168–178. [CrossRef] [PubMed]
25. Ocker, M.; Höpfner, M. Apoptosis-Modulating Drugs for Improved Cancer Therapy. *Eur. Surg. Res.* **2012**, *48*, 111–120. [CrossRef] [PubMed]
26. An, W.; Lai, H.; Zhang, Y.; Liu, M.; Lin, X.; Cao, S. Apoptotic Pathway as the Therapeutic Target for Anticancer Traditional Chinese Medicines. *Front. Pharmacol.* **2019**, *10*, 758. [CrossRef]
27. Chao, X.; Wang, G.; Tang, Y.; Dong, C.; Li, H.; Wang, B.; Wu, J.; Zhao, J. The effects and mechanism of peiminine-induced apoptosis in human hepatocellular carcinoma HepG2 cells. *PLoS ONE* **2019**, *14*, e0201864. [CrossRef]
28. Obeng, E. Apoptosis (programmed cell death) and its signals—A review. *Braz. J. Biol.* **2021**, *81*, 1133–1143. [CrossRef]
29. Elmore, S. Apoptosis: A review of programmed cell death. *Toxicol. Pathol.* **2007**, *35*, 495–516. [CrossRef]
30. Han, S.I.; Kim, Y.S.; Kim, T.H. Role of apoptotic and necrotic cell death under physiologic conditions. *BMB Rep.* **2008**, *41*, 1–10. [CrossRef]
31. Alenzi, F.Q. Links between apoptosis, proliferation and the cell cycle. *Br. J. Biomed. Sci.* **2004**, *61*, 99–102. [CrossRef]
32. Bai, J.; Li, Y.; Zhang, G. Cell cycle regulation and anticancer drug discovery. *Cancer Biol. Med.* **2017**, *14*, 348–362.
33. Alimbetov, D.; Askarova, S.; Umbayev, B.; Davis, T.; Kipling, D. Pharmacological Targeting of Cell Cycle, Apoptotic and Cell Adhesion Signaling Pathways Implicated in Chemoresistance of Cancer Cells. *Int. J. Mol. Sci.* **2018**, *19*, 1690. [CrossRef] [PubMed]
34. Fadok, V.A.; Bratton, D.L.; Frasch, S.C.; Warner, M.L.; Henson, P.M. The role of phosphatidylserine in recognition of apoptotic cells by phagocytes. *Cell Death Differ.* **1998**, *5*, 551–562. [CrossRef] [PubMed]
35. Shlomovitz, I.; Speir, M.; Gerlic, M. Flipping the dogma—Phosphatidylserine in non-apoptotic cell death. *Cell Commun. Signal.* **2019**, *17*, 139. [CrossRef] [PubMed]
36. Gross, A.; McDonnell, J.M.; Korsmeyer, S.J. BCL-2 family members and the mitochondria in apoptosis. *Genes Dev.* **1999**, *13*, 1899–1911. [CrossRef] [PubMed]
37. Cheng, E.H.; Wei, M.C.; Weiler, S.; Flavell, R.A.; Mak, T.W.; Lindsten, T.; Korsmeyer, S.J. BCL-2, BCL-X(L) sequester BH3 domain-only molecules preventing BAX- and BAK-mediated mitochondrial apoptosis. *Mol. Cell.* **2001**, *8*, 705–711. [CrossRef]
38. Wei, M.C.; Zong, W.X.; Cheng, E.H.; Lindsten, T.; Panoutsakopoulou, V.; Ross, A.J.; Roth, K.A.; MacGregor, G.R.; Thompson, C.B.; Korsmeyer, S.J. Proapoptotic BAX and BAK: A requisite gateway to mitochondrial dysfunction and death. *Science* **2001**, *292*, 727–730. [CrossRef]
39. Yu, P.; Liu, Q.; Liu, K.; Yagasaki, K.; Wu, E.; Zhang, G. Matrine suppresses breast cancer cell proliferation and invasion via VEGF-Akt-NFkappaB signaling. *Cytotechnology* **2009**, *59*, 219–229. [CrossRef]
40. Zou, J.; Ran, Z.H.; Xu, Q.; Xiao, S.D. Experimental study of the killing effects of oxymatrine on human colon cancer cell line SW1116. *Chin. J. Dig. Dis.* **2005**, *6*, 15–20. [CrossRef]
41. Jin, H.; Sun, Y.; Wang, S.; Cheng, X. Matrine activates PTEN to induce growth inhibition and apoptosis in V600EBRAF harboring melanoma cells. *Int. J. Mol. Sci.* **2013**, *14*, 16040–16057. [CrossRef]
42. Zhang, S.; Qi, J.; Sun, L.; Cheng, B.; Pan, S.; Zhou, M.; Sun, X. Matrine induces programmed cell death and regulates expression of relevant genes based on PCR array analysis in C6 glioma cells. *Mol. Biol. Rep.* **2009**, *36*, 791–799. [CrossRef]
43. Ling, Q.; Xu, X.; Wei, X.; Wang, W.; Zhou, B.; Wang, B.; Zheng, S. Oxymatrine induces human pancreatic cancer PANC-1 cells apoptosis via regulating expression of Bcl-2 and IAP families, and releasing of cytochrome c. *J. Exp. Clin. Cancer Res.* **2011**, *30*, 66. [CrossRef] [PubMed]
44. Song, G.; Luo, Q.; Qin, J.; Wang, L.; Shi, Y.; Sun, C. Effects of oxymatrine on proliferation and apoptosis in human hepatoma cells. *Colloids Surf. B Biointerfaces* **2006**, *48*, 1–5. [CrossRef] [PubMed]
45. Zhang, J.Q.; Li, Y.M.; Liu, T.; He, W.T.; Chen, Y.T.; Chen, X.H.; Li, X.; Zhou, W.C.; Yi, J.F.; Ren, Z.J. Antitumor effect of matrine in human hepatoma G2 cells by inducing apoptosis and autophagy. *World J. Gastroenterol.* **2010**, *16*, 4281–4290. [CrossRef]
46. Yu, H.; Zhu, B.; Yang, W.; Zhang, Q.; Wang, W.; Zhai, W.; Lu, L.; Zheng, Y.; Dang, Z.; Li, B.; et al. Matrine inhibits proliferation and migration of HepG2 cells by downregulating ERK1/2 signaling pathways. *J. Cancer Res. Ther.* **2020**, *16*, 209–214. [PubMed]
47. Chen, K.; Zhu, P.; Ye, J.; Liao, Y.; Du, Z.; Chen, F.; He, J.; Zhang, S.; Zhai, W. Oxymatrine inhibits the migration and invasion of hepatocellular carcinoma cells by reducing the activity of MMP-2/-9 via regulating p38 signaling pathway. *J. Cancer* **2019**, *10*, 5397–5403. [CrossRef]